



## Effect of Opening Geometry on Full-Scale Internal Pressure Measurements

Mitchell Humphreys<sup>1</sup>, John Ginger<sup>2</sup>, David Henderson<sup>3</sup>

<sup>1,2,3</sup>Cyclone Testing Station, James Cook University, Townsville, QLD, 4811, Australia

<sup>1</sup>[mitchell.humphreys@my.jcu.edu.au](mailto:mitchell.humphreys@my.jcu.edu.au)

<sup>2</sup>[john.ginger@jcu.edu.au](mailto:john.ginger@jcu.edu.au)

<sup>3</sup>[david.henderson@jcu.edu.au](mailto:david.henderson@jcu.edu.au)

### ABSTRACT

An opening in a building envelope can cause large internal pressures, which are crucial to structural design of buildings. Analytical methods used to describe internal pressure fluctuations utilize ill-defined parameters, particularly loss and inertial coefficients,  $C_L$  and  $C_I$ . This paper focuses on the full-scale experimental setup used to record internal and external pressures under atmospheric wind flow to validate analytical methods. Typical resonance of internal pressure fluctuations was observed. Spectral matching was used to define loss and inertial coefficients for opening area to volume ratios,  $\Phi_1 (= A^{3/2}/V)$ ,  $28 \times 10^{-6}$ ,  $48 \times 10^{-6}$  and  $222 \times 10^{-6}$  at relatively large  $\Phi_5 (= \lambda_{in}/\sqrt{A})$  values. Results indicate  $C_L$  increases with  $\Phi_1$ , ranging between 8.5 and 30, where  $C_I$  ranged from 1.25 to 1.7.

### 1. Introduction

Openings in the building envelope have the potential to generate large internal pressures during strong winds, contributing to a significant proportion of the net pressures across the envelope. Such scenarios are a common cause of structural failure during windstorms and typically become the critical loading criterion for structural design (Walker (1974)). Thus, accurate prediction of internal pressures is critical to building reliable and affordable structures.

Wind induced internal pressures have been shown to be dependent on several key parameters, approach wind characteristics, external pressure field, size and location of openings, envelope flexibility and volume. Theoretical and experimental studies over the past 40 years have examined these parameters. Particular attention has been given to single large openings on the windward face, as this is generally the critical design case.

Holmes (1979), Vickery (1986), Sharma and Richards (1997) are among those who have developed second-order nonlinear differential equations, which describe internal pressure fluctuations with a single large opening. Internal pressure fluctuations in buildings that are nominally sealed have also been studied. However, validation of these methods is limited due to difficulties associated with measuring internal pressures at full-scale. This study focuses on the measurement of full-scale internal and external pressures with the aim to provide a theoretical basis for the validation of analytical methods.

Holmes (1979) described internal pressure fluctuations caused by external pressures applied to a single opening using the Helmholtz resonator model, given in Equation 1. Here an effective slug of air moves in and out of the building with momentum, damping and background resistance. The terms read left to right as the inertial, damping, background stiffness and driving force.

$$\frac{C_I V}{a_s^2 \sqrt{A}} \ddot{p}_i + \frac{C_L}{2\rho} \left( \frac{V}{a_s^2 A} \right)^2 \dot{p}_i |\dot{p}_i| + p_i = p_e \quad (1)$$

Here  $p_i$  and  $p_e$  are the internal and external pressure at the opening varying with time  $t$ ,  $\dot{p}_i$  and  $\ddot{p}_i$  are first and second time derivatives of  $p_i$ .  $A$  is the opening area,  $a_s$  is the speed of sound,  $V$  is the effective building volume,  $\rho$  is the density of air, and  $C_L$  and  $C_I$  are the loss and inertial coefficients.

The characteristics of internal and external pressure fluctuations can be studied by their spectral densities,  $S_{p_i}(f)$  and  $S_{p_e}(f)$  respectively. Assuming linearity,  $S_{p_i}(f)$  can be related to  $S_{p_e}(f)$  with a frequency dependent admittance function,  $|x_{i/e}|^2$ , where  $S_{p_i}(f) = |x_{i/e}|^2 S_{p_e}(f)$ . Internal pressure resonance occurs at Helmholtz frequency,  $f_H$ , given in Equation 2, and is primarily dependent on the opening area to volume ratio and  $C_I$ . As volume increases or opening area decreases, dampening in Equation 1 increases, and  $f_H$  decreases, thus the effect of internal pressure is not clear.

$$f_H = \frac{1}{2\pi} \sqrt{\frac{a_s^2 \sqrt{A}}{C_I V}} \quad (2)$$

Vickery and Bloxham (1992) indicated that  $C_L$  and  $C_I$  can only be defined for limited situations such as one directional uniform flow passing through a sharp edged circular opening connecting two large volumes, where potential flow theory gives  $C_L = ((\pi + 2)/\pi)^2 = 2.68$ , and  $C_I = \sqrt{\pi/4} = 0.89$ . Reviews on internal pressures in buildings by Holmes and Ginger (2012) and Sharma (2012) show that many researchers have derived  $C_I$  between 0.8 and 1.55 and  $C_L$  between 2.5 to 100, most via spectral matching. Here the finite difference method is used to solve for internal pressure in Equation 1, and a simulated internal pressure signal is manufactured, its spectra is then matched with the measured internal pressure spectra in an iterative process by adjusting  $C_L$ . Sharma (2012) illustrated that utilizing a range of loss and inertial coefficients in use, predicted fluctuating and peak internal pressures can vary by 40%, illustrating the importance of this issue. Ginger *et al.* (2010) proposed that  $C_L$  isn't constant and changes with respect to non-dimensional parameters:  $\Phi_1 = A^{3/2}/V$ , opening area to volume,  $\Phi_2 = a_s/\bar{U}$ , speed of sound to mean wind speed, and  $\Phi_5 = \lambda_u/\sqrt{A}$ , integral length scale of turbulence to opening area. This study focuses on the acquisition of full-scale internal pressures in a well-sealed volume with a single opening to validate these analytical methods.

## 2. Full-Scale Testing Methodology

A system was developed to measure full-scale external and internal pressures on a 6m long  $\times$  2.4m wide  $\times$  2.5m high enclosed shipping container at JCU Townsville under atmospheric wind flow, shown in Figure 1a. A 2.4m  $\times$  2.5m ridged plywood partition was installed in the doorway to seal the container, establishing a volume of 36m<sup>3</sup>, in which a range of opening types/sizes can be installed. External pressure taps were positioned around the opening as shown in Figure 1b. Internal pressure was measured 1.5m from the opening. Pressure transducers were referenced to atmospheric pressure obtained 20m from the shipping container in a sealed 20L bucket with a flat lid flush with the ground. Four 12mm holes on the surface allow for changes in atmospheric pressure.



Figure 1. a) Shipping container with partition b) External pressure taps around opening

Pressures were recorded at 200Hz for 10 minute intervals, a solenoid valve was used to zero the transducers at the beginning of each run, signals are then low pass filtered to 15Hz. Honeywell TruStability® differential pressure transducers with ranges of  $\pm 500\text{Pa}$  and  $\pm 2500\text{Pa}$  were used to measure internal and external pressures. The pressure transducers were connected to the pressure taps via 0.2m of 4mm diameter vinyl tubing and a 3-way solenoid valve with a flow coefficient of 0.19. The Data Acquisition system (DAQ) used was a National Instruments Compact DAQ 9137 with analog input module NI9205. An RM young anemometer collected wind speed and directionality at a height of 3m, 10m from the opening. Signal distortion due to the addition of tubing and solenoid was examined, the results showed unit gain and zero phase lag below 15Hz. Turbulent Flow Instrumentation Dynamic Pressure Measurement System was used to check pressure transducer calibration up to their maximum and minimum ranges or  $\pm 1.3\text{kPa}$ , whichever was greater.

Tests were carried out for the configurations given in Table 1. Data from natural approach wind flow is limited by the available windy days, and constraints on resources. Site winds speed data was only collected for case 2, estimates from the Townsville airport are given for cases 1 and 3. Wind flow normal to the face with the opening is defined as direction  $0^\circ$ .  $\Phi_1$  and  $\Phi_5$  values are also given in Table 1 estimating  $\lambda_u = 100\text{m}$ . Typical  $\Phi_1$  values for a building can range from 0.2 to  $1 \times 10^{-6}$ , however typical  $\Phi_5$  values range from 20 to 200.  $\Phi_5$  values given in Table 1 are not within this range suggesting the external pressure fluctuations are well correlated over the opening in these experiments compared to buildings with similar  $\Phi_1$  values.

Table 1. Opening Configurations

Case #	Opening (mm×mm)	Area ( $\times 10^{-3}\text{m}^2$ )	Thickness (mm)	$\Phi_1 = A^{3/2}/V$ ( $\times 10^{-6}$ )	$\Phi_5 = \lambda_u/\sqrt{A}$	Time (min)	$\bar{U}$ (m/s)	Mean Dir. ( $^\circ$ )
1	200×200	40	19	222	500	0.85	$\approx 2.5$	$\approx 10^\circ$
2	120×120	14.4	5	48	833	8.0	$\approx 2.5$	$\approx 30^\circ$
3	100×100	10	5	28	1000	4.1	$\approx 2.5$	$\approx 10^\circ$

Additional experiments that apply simulated external pressure fluctuations to the same experimental setup using pressure loading actuators are also being conducted. The aim of these tests is to study the response of internal pressures to a range of additional parameters with repeatable external pressure fluctuations that can range in magnitude and applied pressure fluctuations.

## 5. Results and Discussion

Figures 3 to 5 show 50 and 10 seconds of external, internal and net (external - internal) pressure data. Figures 3 and 5 show positive pressures as the winds were relatively perpendicular to the opening. Figure 4 shows generally negative pressures as the winds were more oblique (i.e. opening on side wall).

Figure 3 to 5 show that the internal pressure follows the external pressure for all cases irrespective of opening size, with the net pressure across the opening fluctuating about zero. The internal pressure in Figure 3 overshoots the external pressure leading into oscillations of internal and net pressure (i.e. between 16 and 18 seconds). Figure 5 shows net pressures greater than or less than 0Pa for significant lengths of time, without internal pressure overshooting and oscillations. Figure 4 may have sustained more oblique flow possibly causing grazing flow across the opening, however the internal pressure response is similar to Figures 3 and 5, with less defined overshoots and oscillations than Figure 3, and lower peak net pressures than Figure 5.

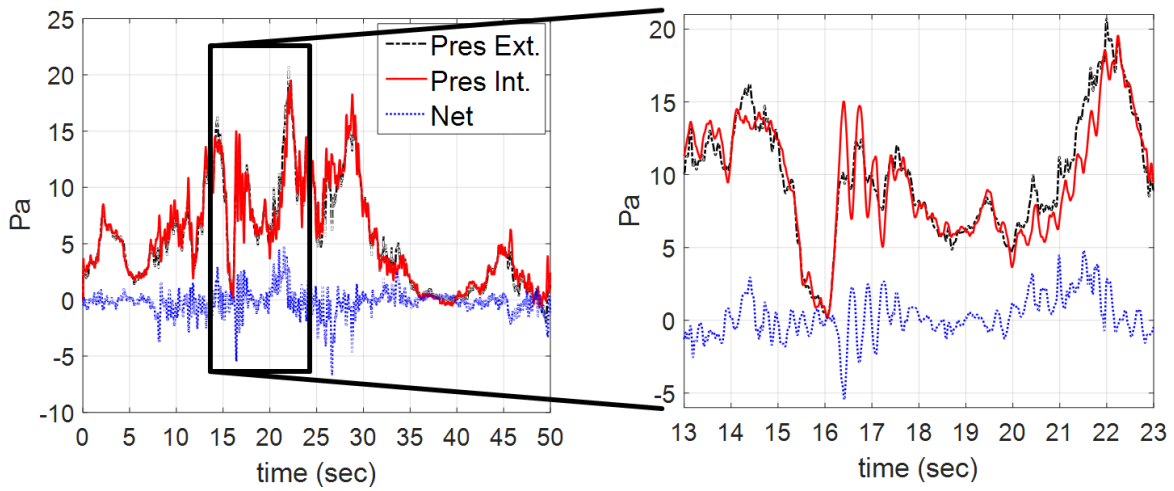


Figure 3. Case 1: External, Internal and Net Pressure

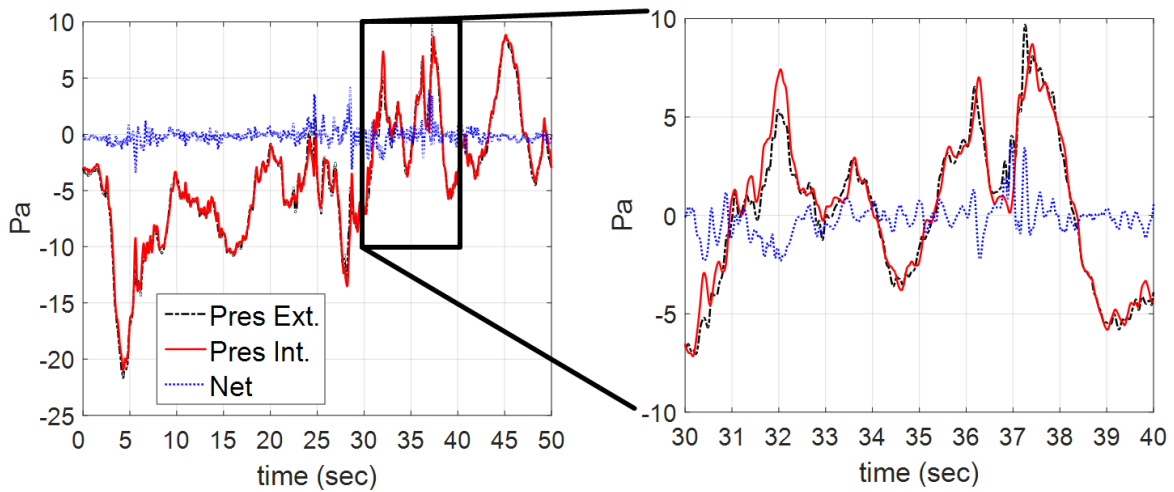


Figure 4. Case 2: External, Internal and Net Pressure

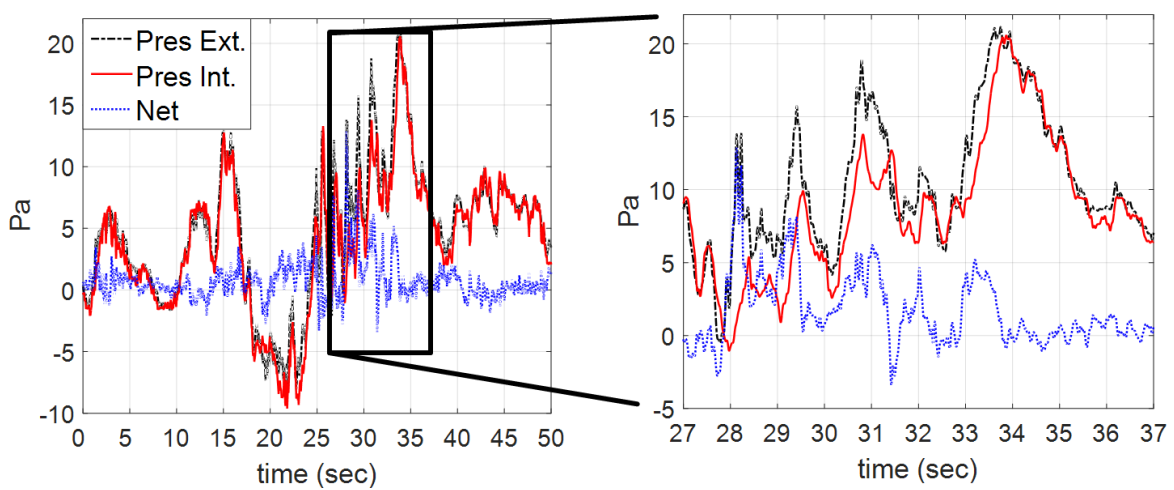


Figure 5. Case 3: External, Internal and Net Pressure

The external, internal and simulated internal pressure spectra of the three cases are shown in Figures 6a) to 6c). The frequency dependent admittance function,  $|x_{i/e}|^2$ , is also given in Figure 6. Due to shorter sampling time of case 1, Figure 6a) appears unstable compared to Figures 6b) and 6c), however, results are still comparable as each case had similar mean wind speeds.

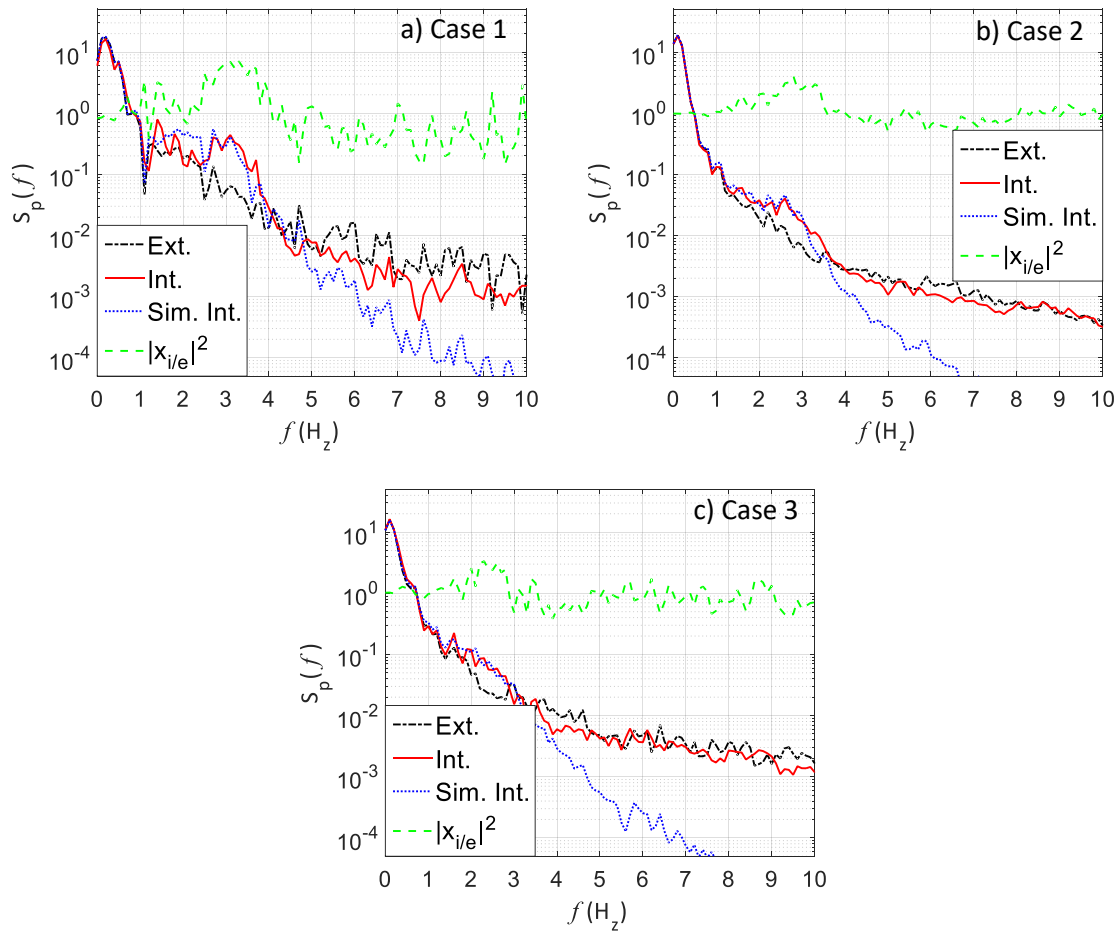


Figure 6. External, Internal, Simulated Spectra and Admittance Function

Helmholtz frequency,  $f_H$ , is shown in each case by the increase in internal pressure fluctuations. The value of  $f_H$  is taken as the frequency  $|x_{i/e}|^2$  is at its greatest.  $C_L$  is derived using Equation 2, and  $C_I$  is derived via spectral matching, values are given in Table 2. The admittance function shows a decrease in resonance with decreasing  $\Phi_1$ , similar to model scale studies by Yu *et al.* (2008), Ginger *et al.* (2010), Guha *et al.* (2013) and Xu *et al.* (2016). Internal pressure fluctuations in all three cases remain similar to the external fluctuations after Helmholtz frequency, unlike most model-scale wind tunnel studies, this is due to the close proximity of the external pressure taps to the opening and large scale of  $\Phi_5$  ( $= \lambda_u/\sqrt{A}$ ).

Table 2. Loss and Inertial Coefficients derived from spectral matching

Case #	Opening (mm×mm)	$\Phi_1 = A^{3/2}/V$ ( $\times 10^{-6}$ )	$C_L$	$C_I$	$f_H$ (Hz)	$ x_{i/e} ^2$ at $f_H$
1	200×200	222	30	1.7	3.1	7
2	120×120	48	13	1.25	2.8	4
3	100×100	28	8.5	1.3	2.5	3.4

## 4. Conclusions

A full-scale experimental setup to measure internal and external pressures on an enclosed 36m<sup>3</sup> volume with a single opening under atmospheric flow is presented. Three different single opening sizes were tested, typical Helmholtz resonance was recorded. Loss and inertial coefficients were derived using spectral matching, with  $C_L$  between 8.5 to 30, and  $C_I$  between 1.25 to 1.7. The magnitude of the resonant peak at Helmholtz frequency decreased with decreasing opening area to volume ratio similar to model scale studies. This study focused on the measurement of full-scale internal and external pressures to validate analytical methods, having demonstrated this, additional testing will be conducted.

## Acknowledgments

The authors gratefully acknowledge the support of the Commonwealth of Australia through the cooperative Research Centre program and Australian Research Council linkage grant, Australasian Steel Institute Ltd, JDH Consulting and Scott Woolcock Consulting Pty Ltd as industry partners.

## References

- Ginger, J. D., Holmes, J. D., Kim, P. Y. (2010). Variation of internal pressure with varying sizes of dominant openings and volumes. *Journal of Structural Engineering*, 136(10), 1319-1326.
- Guha, T. K., Sharma, R. N., Richards, P. J. (2014). Internal pressure in a building with a single dominant opening: an experimental and numerical case study. *Journal of Structural Engineering (Mandras)*, 41, 59-67.
- Holmes, J. D. (1979). Mean and fluctuating internal pressures induced by wind. *Proceedings of the Fifth International Conference on Wind Engineering*, Fort Collins, Colorado, USA, 1979, Peragmon Press, Oxford, 1980, 435-450
- Holmes, J. D., Ginger, J. D. (2012). Internal pressures - The dominant windward opening case - A review. *Journal of Wind Engineering and Industrial Aerodynamics*, 100(1), 70-76.
- Sharma, R. N. (2012). The ill-defined parameters of the building internal pressure dynamics problem. *Proceedings of the the 18th Australasian Fluid Mechanics Conference*, Launceston, Tasmania, Australia, Dec 3-7, 2012. 4pp.
- Sharma, R. N., Richards, P. J. (1997). The effect of roof flexibility on internal pressure fluctuations. *Journal of Wind Engineering and Industrial Aerodynamics*, 72, 175-186.
- Vickery, B. J. (1986). Gust-Factors for Internal-Pressures in Low Rise Buildings. *Journal of Wind Engineering and Industrial Aerodynamics*, 23(1-3), 259-271.
- Vickery, B. J., Bloxham, C. (1992). Internal pressure dynamics with a dominant opening. *Journal of Wind Engineering and Industrial Aerodynamics*, 41(1-3), 193-204.
- Walker, G. R. (1975), Report On Cyclone 'Tracy': Effect On Buildings, *Australian Department of Housing and Construction*.
- Xu H. W., Yu S. C., Lou W. J. (2016) Estimation Method of Loss Coefficient for Wind-Induced Internal Pressure Fluctuations, *Journal of Engineering Mechanics*, 142(7), 04016041.
- Yu S. C., Lou W. J., Sun B. N. (2008). Wind-induced internal pressure response for structure with single windward opening and background leakage, *Journal of Zhejiang University-SCIENCE A*, 9(3), 313-321.